Nonlinear Resonances and Chaotic Behavior in a Periodically Focused Intense Charged-Particle Beam

Chiping Chen
Plasma Fusion Center, Massachusetts Institute of Technology, Cambridge, Massachusetts 02139

Ronald C. Davidson
Plasma Physics Laboratory, Princeton University, Princeton, New Jersey 08543
(Received 27 December 1993)

It is shown that beam self-field effects induce nonlinear resonances and chaotic behavior in the envelope oscillations of an intense charged-particle beam propagating through a periodic focusing field. The resonance condition is derived and expressed in terms of the vacuum phase advance and the beam perveance. Certain correlations are found between such resonant and chaotic behavior and well-known instabilities in periodically focused high-current ion beams. The predicted nonlinear resonances and chaotic behavior are expected to be observable in beam transport experiments in which there is a mismatch between the beam and the periodic focusing field.

PACS numbers: 41.85.Ja, 05.45.+b, 29.27.Eg, 52.25.Wz

The physics of periodically focused intense charged-particle beams has been studied since the late 1950s [1-3]. The need for an advance in understanding has intensified recently, because many advanced accelerator applications, such as free-electron lasers [4], heavy ion fusion [5], and nuclear waste treatment, require high-brightness (i.e., high current and low emittance) electron and ion beams. Several critical aspects of intense charged-particle beam transport in a periodic focusing channel have been investigated theoretically and experimentally, including (i) exploration of the equilibrium [1] and stability [2] properties of intense beams, (ii) introduction of the concept of root-mean-squared (rms) emittance [6-8], (iii) derivation of the rms beam envelope equations [6,7,9], (iv) study of current intensity limits [10], and (v) exploration of the emittance growth [11-15] and beam halo phenomena. Despite these efforts, a *basic* understanding of the physics of intense charged-particle beam propagation in a periodic focusing channel has not yet emerged, particularly in the regime where the beam is mismatched into the focusing channel.

In this Letter, we report two new phenomena in periodically focused intense charged-particle beams, namely, beam self-field-induced nonlinear resonances, and chaotic behavior in the beam envelope oscillations. In particular, the evolution of the envelope of an intense beam in a periodic solenoidal focusing field is studied. The Poincaré mapping technique is used to find the condition for beam matching into the focusing channel and to explore the nonlinear resonances and chaotic behavior in the envelope oscillations of mismatched beams. The nonlinear resonances, which can be classified in terms of the vacuum phase advance and a scaled, normalized beam perveance, are correlated with well-known instabilities [2] in periodically focused high-current ion beams with the Kapchinskij-Vladimirskij (KV) equilibrium distribution [1]. As the vacuum phase advance and beam current are increased, highly chaotic beam envelope oscillations are found for beams that are not closely into the periodic focusing channel.

We describe the envelope oscillations of an intense charged-particle beam propagating through the periodic solenoidal focusing field $\mathbf{B}(r,s)$ by [1,3,6,16]

$$\frac{d^2 r_b}{ds^2} + \kappa_z(s) r_b - \frac{K}{r_b} - \frac{\epsilon^2}{r_b^3} = 0 \qquad (1)$$

in the paraxial approximation. In the beam envelope equation (1), r_b is the beam radius and $s = z = \beta_b ct$ is the axial coordinate, where $\beta_b c$ is the average axial velocity of the beam particles, and c is the speed of light *in vacuo*. The periodic function $\kappa_z(s) = \kappa_z(s+S) = q^2 B_z^2(s)/4\gamma_b^2\beta_b^2 m^2 c^4$ characterizes the strength of the focusing field, where $B_z(s) = B_z(0,s)$ is the magnetic field on the z axis, S is the fundamental periodicity length of the focusing field, q and m are the particle charge and rest mass, respectively, and $\gamma_b = (1-\beta_b^2)^{-1/2}$ is the relativistic mass factor of the beam particles. The periodic step-function profile shown in Fig. 1 is assumed for $\kappa_z(s)$, and the vacuum phase advance over one axial period of such a focusing field is given approximately by $\sigma_0 = [S\int_0^S \kappa_z(s)ds]^{1/2} = [\eta S^2 \kappa_z(0)]^{1/2}$. The normalized beam perveance $K = 2q^2 N_b/\gamma_b^3 \beta_b^2 mc^2$ is a measure of the beam self-field [3] intensity, where N_b is the number of particles per unit axial length of the beam.

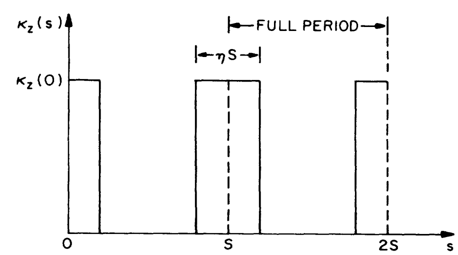

FIG. 1. Periodic step-function lattice $\kappa_z(s)$ representing a periodically interrupted or alternating solenoidal focusing field.

Equation (1) can be regarded as either a rigorous differential equation governing the evolution of the outermost radius (envelope) of a beam with KV distribution function [1,3,16] or a phenomenological model describing the evolution of the beam radius in an rms sense [6]. For a beam with KV distribution function, it can be shown [16] that the emittance is given by $\epsilon = 2P_{\theta m}/\gamma_b m\beta_b c$ =const, where $P_{\theta m}$ is the maximum canonical angular momentum achieved by the beam particles. In the phenomenological model [6], $r_b/\sqrt{2}$ is the rms beam radius, and ϵ is the rms emittance which generally varies with s but is assumed to be *constant* in the present analysis. For a beam in the saturated state of emittance growth, such an assumption is well justified.

In the limit of *tenuous* beam with $K \to 0$, Eq. (1) is integrable because it is equivalent to the *linear* second-order ordinary differential equation $d^2u/ds^2 + \kappa_z(s)u = 0$ by means of the transformation $u(s) = r_b(s)\cos[\epsilon\int_0^s ds/r_b^2(s) + \Psi_0]$. For a symmetric lattice with $\kappa_z(s) = \kappa_z(s+S) = \kappa_z(-s)$, such a linear differential equation is known as Hill's equation. Furthermore, in the limit of a *uniform* magnetic field with $\kappa_z(s) = \kappa_{z0}$=const, Eq. (1) is also integrable, because the oscillations occur in the effective one-dimensional static potential well described by $V(r_b) = k_{z0}r_b^2/2 - K\ln r_b + \epsilon^2/2r_b^2$. The potential $V(r_b)$ has a unique minimum at

$$r_b(s) = r_{b0} = \left\{ \left[\left(\frac{K}{2\kappa_{z0}} \right)^2 + \frac{\epsilon^2}{\kappa_{z0}} \right]^{1/2} + \frac{K}{2\kappa_{z0}} \right\}^{1/2}, \quad (2)$$

which determines the radius of a matched (equilibrium) beam for the case of a uniform magnetic field. As K is increased, the beam radius expands due to the (defocusing) self-field effect. Indeed, as $K/\epsilon\kappa_{z0}^{1/2} \to \infty$, Eq. (2) recovers the *Brillouin flow condition* [3], i.e., $2\omega_{pb}^2/\gamma_b\omega_c^2 = 1$, where $\omega_{pb} = (4q^2N/mr_{b0}^2)^{1/2}$ is the nonrelativistic plasma frequency of the beam particles, and $\omega_c = qB_z/mc$ is the nonrelativistic cyclotron frequency.

For $d\kappa_z/ds \neq 0$ and sufficiently large K, however, the beam envelope equation (1) describes a Hamiltonian system with one and one-half degrees of freedom. It will be shown in the subsequent analysis that Eq. (1) is *nonintegrable* and that the beam self-field effects induce *nonlinear resonances* and *chaotic behavior* in the beam envelope oscillations. To parametrize Eq. (1) effectively, we introduce the *dimensionless* parameters and variables defined by

$$\frac{s}{S} \to s, \quad \frac{r_b}{\sqrt{\epsilon S}} \to r_b, \quad S^2\kappa_z \to \kappa_z, \quad \frac{SK}{\epsilon} \to K, \quad (3)$$

and express Eq. (1) in the normalized form

$$\frac{d^2r_b}{ds^2} + \kappa_z(s)r_b - \frac{K}{r_b} - \frac{1}{r_b^3} = 0, \quad (4)$$

which is now characterized by the two dimensionless parameters K and $\kappa_z(s)$. Unless specified otherwise, the dimensionless parameters and variables defined in Eq. (3) will be used in the remainder of this paper.

To explore the nonlinear resonances and demonstrate chaotic behavior in the beam envelope oscillations, we use the *Poincaré mapping technique* [17] to track an ensemble of phase-space trajectories as they intersect the phase plane (r_b, r_b') located at successive axial positions $s = 0, 1, 2, \ldots$, where $r_b' = dr_b/ds$. Formally, such a map is expressed as

$$\begin{pmatrix} r_b \\ r_b' \end{pmatrix}_{n+1} = \mathrm{T}\begin{pmatrix} r_b \\ r_b' \end{pmatrix}_n = \begin{pmatrix} \zeta(r_b, r_b') \\ \xi(r_b, r_b') \end{pmatrix}_n, \quad n = 0, \pm 1, \pm 2, \ldots, \quad (5)$$

which maps the phase plane (r_b, r_b') onto itself from $s = n$ to $s = n+1$. In the present analysis, the functions $\zeta(r_b, r_b')$ and $\xi(r_b, r_b')$ are obtained implicitly by integrating Eq. (4) numerically with a fourth-order Runge-Kutta algorithm.

The axial dependence of the radius of a matched (equilibrium) beam corresponds to a *periodic solution* [i.e., $r_b(s+1) = r_b(s)$] to Eq. (4), which in turn corresponds to a *fixed point* of the map defined by

$$\begin{pmatrix} \bar{r}_b \\ \bar{r}_b' \end{pmatrix} = \mathrm{T}\begin{pmatrix} \bar{r}_b \\ \bar{r}_b' \end{pmatrix}. \quad (6)$$

In principle, such a fixed point may correspond to a periodic solution with a fundamental periodicity of $1/N$, where $N = 1, 2, \ldots$. A fixed point is *stable* if the eigenvalues of the tangent map about that fixed point are of unit module.

The Poincaré map T has the property that for a *symmetric* lattice with $\kappa_z(s) = \kappa_z(s+1) = \kappa_z(-s)$, such as the periodic step-function profile shown in Fig. 1, the line $r_b' = 0$ (r_b axis) is an axis of symmetry of the map T; that is, the phase plane (r_b, r_b') is symmetric with respect to the r_b axis. This symmetry follows from the fact that Eq. (4) is invariant under the transformation $(s, r_b, r_b') \to (-s, r_b, -r_b')$. Moreover, it can be shown that the fixed point of the map corresponds to an intersection of the r_b axis and its image, provided the intersection is unique.

Figure 2(a) shows the Poincaré surface-of-section plot produced by successive applications of T with fifteen initial points along the r_b axis, for a *tenuous* beam in a periodic solenoidal field with step-function lattice (Fig. 1). The choice of system parameters in Fig. 2(a) corresponds to $K = 0$, $\eta = \frac{1}{6}$, and $\kappa_z(0) = 3.79$ ($\sigma_0 = 45.5°$). There is a unique fixed point (i.e., a unique matched beam) at $r_b = \bar{r}_b = 1.1$ on the r_b axis. The fixed point is surrounded by an infinite number of invariant tori, fourteen of which are shown in Fig. 2(a). Each of the tori describes a mismatched (nonequilibrium) beam whose envelope exhibits stable betatron oscillations about the envelope of the matched beam. In general, the envelope oscillations of a mismatched beam consist of the superposition of the envelope oscillations of the corresponding matched beam and the associated betatron oscillations. It should be emphasized that because Eq. (4) is integra-

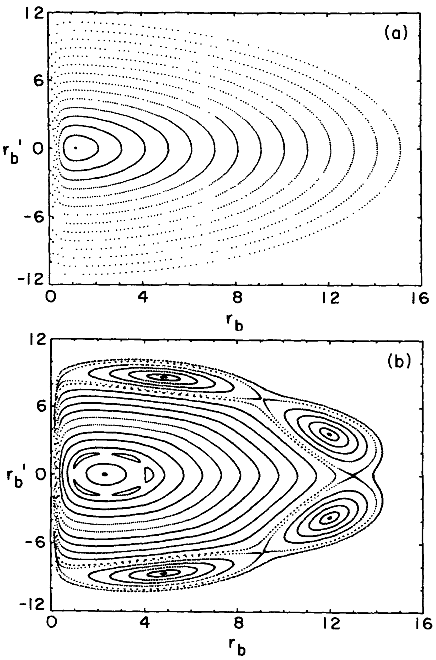

FIG. 2. Poincaré surface-of-section plot for the envelope oscillations of tenuous and intense beams. The choice of system parameters corresponds to (a) $K=0$, $\eta=\frac{1}{6}$, $\kappa_z(0)=3.79$ ($\sigma_0=45.5°$), and (b) $K=3$, $\eta=\frac{1}{6}$, $\kappa_z(0)=3.79$ ($\sigma_0=45.5°$).

ble in the limit of a tenuous beam, there is no finite-size resonance, as illustrated in Fig. 2(a).

For a direct comparison with Fig. 2(a), the corresponding Poincaré surface-of-section plot is shown in Fig. 2(b) for an *intense* beam with normalized self-field perveance $K=3$. It is evident that the rich phase-space structure in Fig. 2(b) is strikingly different from the simple phase-space structure in Fig. 2(a). In particular, there coexist fourth-order resonances (i.e., period-four orbits) and fifth-order resonances (i.e., period-five orbits) in the phase space shown in Fig. 2(b). The stable fifth-order resonance corresponds to the five elliptical regions separated by the unstable fifth-order resonance in the vicinity of the fixed point (i.e., the matched beam) which is located at $r_b=\bar{r}_b=2.3$ and $r_b'=\bar{r}_b'=0$. The corresponding phase advance over one focusing period is evaluated to be $\sigma=\int_0^1 ds/\bar{r}_b^2(s)=0.257\sigma_0=11.7°$, where $\bar{r}_b(s)$ is the s-dependent radius of the matched beam. The stable and unstable fourth-order resonances are further away from the fixed point. Because the nonlinearity is small for the case shown in Fig. 2(b), chaotic behavior is hardly visible near the separatrix of either the fourth-order resonances or the fifth-order resonances.

To characterize the nonlinear resonances such as those shown in Fig. 2(b), we have examined the parametric dependence of the axial wave number of the betatron oscillations. It is found that the fifth-order resonances in Fig. 2(b) consist of betatron oscillations with wave number $k=k_5^{(1)}=2\pi/5$. Similarly, the betatron wave number for the fourth-order resonances is $k=k_4^{(1)}=\pi/2$. In general, for a pair of stable and unstable nth-order resonances, the betatron wave number is given by $k=k_n^{(l)}\equiv 2\pi l/n$, where $l=1,2,\ldots,n-1$.

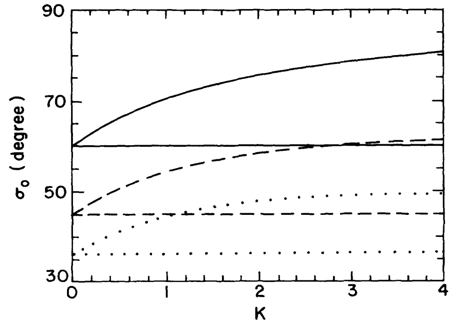

FIG. 3. Parameter domain for the resonances of order $n=3$, 4, and 5 with betatron wave numbers $k_n^{(1)}=2\pi/3$, $\pi/2$, and $2\pi/5$. The third-, fourth-, and fifth-order resonances occur in the regions bounded by the solid, dashed, and dotted curves, respectively.

In the smooth-beam approximation, which is valid for $\sigma_0<90°$, it can be shown that the wave number of small-amplitude betatron oscillations about the matched beam is given by

$$k=k(\sigma_0,K)\equiv[4\sigma_0^2+K^2-K(4\sigma_0^2+K^2)^{1/2}]^{1/2}, \quad (7)$$

where $\sigma_0=[\int_0^1 ds\kappa_z(s)]^{1/2}=[\eta\kappa_z(0)]^{1/2}$ is the vacuum phase advance, and K is the normalized self-field perveance defined in Eq. (3). On the other hand, for large-amplitude betatron oscillations, the space-charge (third) term in Eq. (4) is negligibly small, and consequently the betatron wave number is approximately $k=k(\sigma_0,K\to 0)=2\sigma_0$. Therefore, for specified values of σ_0 and K, the wave number of arbitrary-amplitude betatron oscillations must satisfy the inequality $2\sigma_0\le k\le k(\sigma_0,K)$. In other words, the parameter domain for existence of the nth-order resonance with betatron wave number $k_n^{(l)}=2\pi l/n$ is determined approximately by the condition

$$\frac{\pi l}{n}\le\sigma_0 \le\left\{\frac{K}{2}\left[\left(\frac{\pi l}{n}\right)^2+\left(\frac{K}{4}\right)^2\right]^{1/2}+\left(\frac{\pi l}{n}\right)^2-\frac{K^2}{8}\right\}^{1/2}, \quad (8)$$

where $n=3,4,5,\ldots$ and $l=1,2,\ldots,n-1$. For $\sigma_0<90°$, the condition expressed in Eq. (8) has been verified by the numerical integration of Eq. (4), and agreement is typically better than 5%. It follows from Eq. (8) that the resonance width is given by $\Delta\sigma_0=(\sqrt{2}-1)\pi l/n$ as $K\to\infty$.

Figure 3 shows the parameter domains for the resonances of order $n=3$, 4, and 5 with $l=1$, as obtained from Eq. (8). The parameter domain for the third-order (fourth-order) resonances overlaps with that for the fourth-order (fifth-order) resonances for sufficiently large values of K, whereas they are well separated for $K<1$.

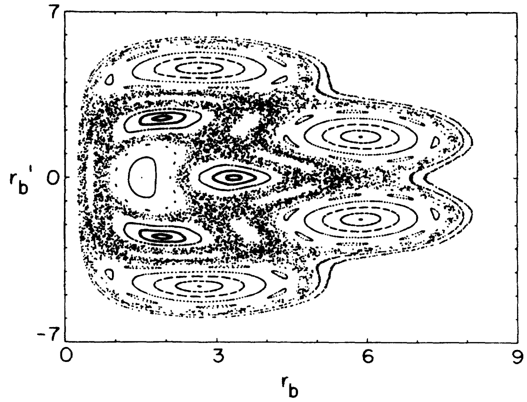

FIG. 4. Poincaré surface-of-section plot of the beam envelope oscillations for the choice of system parameters corresponding to $K=5$, $\eta=\frac{1}{6}$, and $\kappa_z(0)=24.2$ ($\sigma_0=115°$).

This explains why, for $\sigma_0=45.5°$ and $K=3$, the fourth- and fifth-order resonances coexist in the Poincaré surface-of-section plot shown in Fig. 2(b).

For $\sigma_0>90°$ and sufficiently large K, the envelope oscillations become chaotic for some mismatched beams. This is demonstrated by the Poincaré surface-of-section plot shown in Fig. 4 for the choice of system parameters corresponding to $K=5$, $\eta=\frac{1}{6}$, and $\kappa_z(0)=24.2$ ($\sigma=115°$). In contrast to Fig. 2, the phase space now contains regular (elliptical) orbits as well as *chaotic* orbits which are *very sensitive to initial conditions*. In addition to the almost regular region associated with the fixed point at $\bar{r}_b=1.6$ and $\bar{r}_b'=0$, there are stable third- and fourth-order resonances with $k=k_3^{(2)}=4\pi/3$ and $k=k_4^{(2)}=\pi$, respectively. The fixed point is completely engulfed by the chaotic orbits as σ_0 and K are further increased.

It is worthwhile pointing out the qualitative connection between the resonant and chaotic phenomena in the beam envelope oscillations and well-known instabilities [2] in periodically focused intense ion beams with KV distribution function [1]. For example, for $\sigma_0=60°$ and $K>2.6$, the KV equilibrium is unstable against the fourth-order, axisymmetric perturbations proportional to r^4 [2], where $r=(x^2+y^2)^{1/2}$ is the radial distance from the beam axis. This instability coincides with the presence of the fourth-order resonances for $\sigma_0=60°$ and $K>2.6$, as seen from Fig. 3. Furthermore, the strong, second-order (envelope) instability [2] for the KV equilibrium, which occurs over a wide range of values of K when $\sigma_0>90°$, is strongly correlated with the chaotic beam envelope oscillations shown in Fig. 4.

It is possible that the beam self-field-induced nonlinear resonances and chaotic behavior reported in this paper play an important role in the transport of mismatched or multiple beams, where large-amplitude, nonequilibrium beam envelope oscillations and beam halo formation may occur.

To summarize, we have reported two new phenomena induced by self-field effects in periodically focused intense charged-particle beams, namely, nonlinear resonances, and chaotic behavior in the beam envelope oscillations. The resonance condition was derived and expressed in terms of the vacuum phase advance and a scaled, normalized beam perveance. Certain correlations were found between the resonant and chaotic phenomena in the beam envelope oscillations and well-known instabilities in periodically focused intense ion beams with the Kapchinskij-Vladimirskij equilibrium distribution. We believe that such resonant and chaotic phenomena can be observed in beam transport experiments in which the beam is not closely matched into the periodic focusing field. Although these findings have so far been obtained for periodic solenoidal field configurations, they are also expected to occur for alternating-gradient quadrupole magnetic field configurations.

This work was supported by the Department of Energy High Energy Physics Division and by the Office of Naval Research.

[1] I. M. Kapchinskij and V. V. Vladimirskij, in *Proceedings of the International Conference on High Energy Accelerators* (CERN, Geneva, 1959), p. 274.
[2] I. Hofmann, L. J. Laslett, L. Smith, and I. Haber, Part. Accel. **13**, 145 (1983).
[3] R. C. Davidson, *Physics of Nonneutral Plasmas* (Addison-Wesley, Reading, MA, 1990).
[4] C. W. Roberson and P. Sprangle, Phys. Fluids B **1**, 3 (1989).
[5] *Heavy Ion Inertial Fusion*, edited by M. Reiser, T. Godlove, and R. Bangerter, AIP Conf. Proc. No. 152 (AIP, New York, 1986), and references therein.
[6] P. M. Lapostolle, IEEE Trans. Nucl. Sci. **18**, 1101 (1971).
[7] F. J. Sacherer, IEEE Trans. Nucl. Sci. **18**, 1105 (1971).
[8] J. D. Lawson, P. M. Lapostolle, and R. L. Gluckstern, Part. Accel. **5**, 61 (1973).
[9] E. P. Lee and R. K. Copper, Part. Accel. **7**, 83 (1976).
[10] M. Reiser, Part. Accel. **8**, 167 (1978).
[11] J. Struckmeier, J. Klabunde, and M. Reiser, Part. Accel. **15**, 47 (1984).
[12] T. P. Wangler, K. R. Crandall, R. S. Mills, and M. Reiser, IEEE Trans. Nucl. Sci. **32**, 2196 (1985).
[13] O. A. Anderson, Part. Accel. **21**, 197 (1987).
[14] M. Reiser, C. R. Chang, D. Kelne, K. Low, T. Shea, H. Rudd, and I. Haber, Phys. Rev. Lett. **61**, 2933 (1988); I. Haber, D. Kelne, M. Reiser, and H. Rudd, Phys. Rev. A **44**, 5194 (1991).
[15] C. L. Bohn, Phys. Rev. Lett. **70**, 932 (1993).
[16] C. Chen and R. C. Davidson, "Nonlinear Properties of the Kapchinskij-Vladimirskij Equilibrium and Envelope Equation for an Intense Charged-Particle Beam in a Periodic Focusing Field" (to be published).
[17] A. J. Lichtenberg and M. A. Lieberman, *Regular and Chaotic Motion* (Springer-Verlag, New York, 1992), 2nd ed.

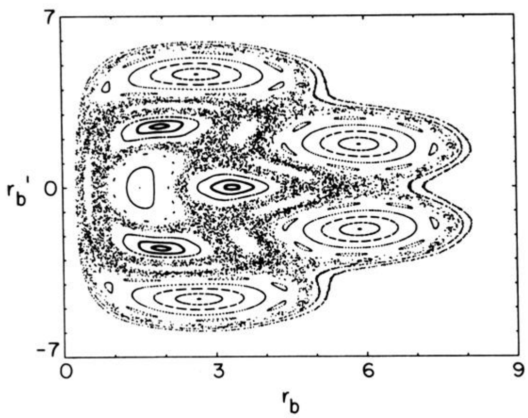

FIG. 4. Poincaré surface-of-section plot of the beam envelope oscillations for the choice of system parameters corresponding to $K=5$, $\eta=\frac{1}{6}$, and $\kappa_z(0)=24.2$ ($\sigma_0=115°$).